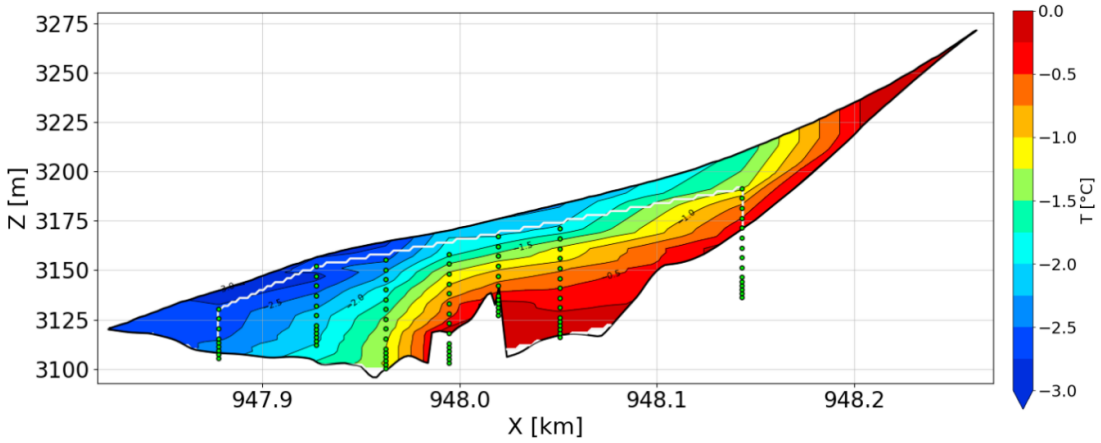

Figure S1. Reconstructed reference temperature field $T = f(x, z)$. The vertical profile is shown along the same longitudinal transect as in Fig. 8 of the main text. Temperatures are assumed uniform in the transverse direction. Green dots represent projections of thermistors used for measurements onto the cross-section. Because the boreholes are not all aligned with the selected transect (see Fig. 1a of the main text), some projected thermistors fall outside of the cross-section outline. The white solid line delineates the region where temperature is interpolated from measurements; outside this area, temperature is extrapolated from the simulation results of Gilbert et al. (2012).

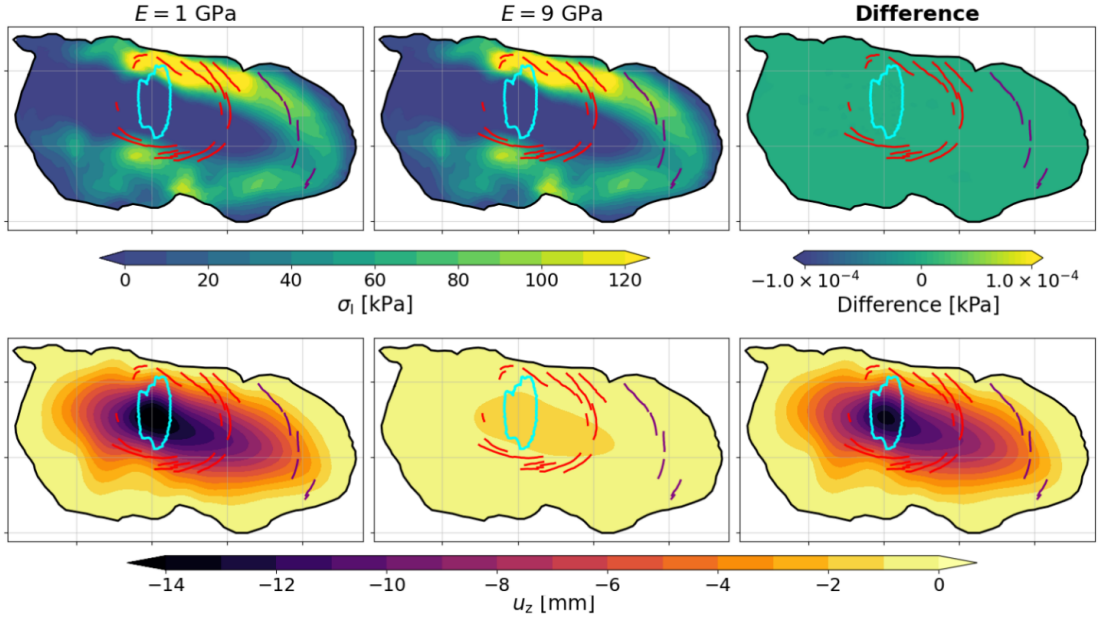

Figure S2. Surface anomalies in (first row) maximum principal stress and (second row) vertical displacement induced by the presence of an empty cavity, modeled using a linear elastic constitutive law with (left column) $E = 1$ GPa and (middle column) $E = 9$ GPa. The right column in each row shows the difference between the results from the two Young's modulus values. Note that a different color scale is used for stress differences (right column, top row), while the same scale is applied across all columns for displacement.

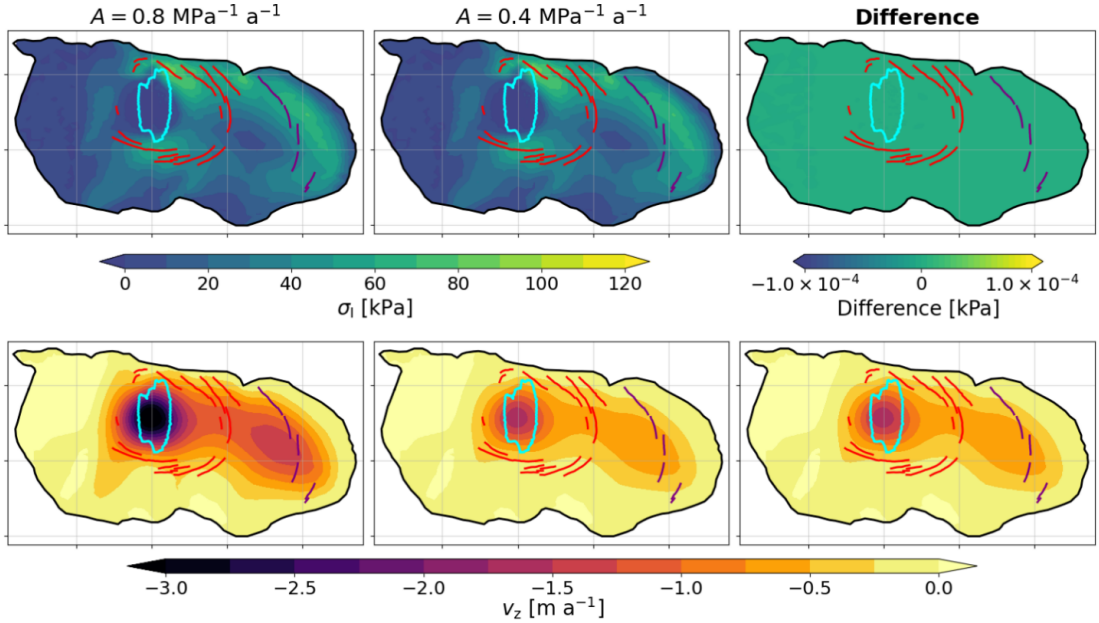

Figure S3. Same as Fig. S2, but for the linear viscous consitutive law with (left column) $A = 0.8$ MPa^{-1} a^{-1} and (middle column) $A = 0.4$ MPa^{-1} a^{-1}. The right column shows the difference between the results from the two fluidity values. Note that, in this case, the second row displays anomalies in vertical velocity rather than vertical displacement as in the elastic case.

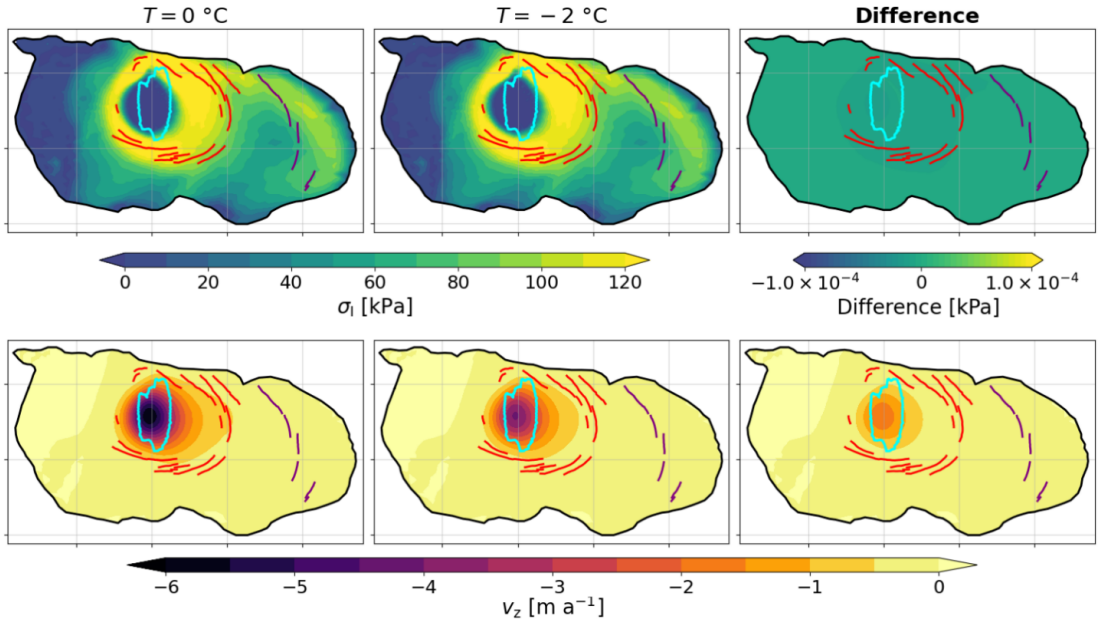

Figure S4. Same as Fig. S3, but for the non-linear Glen's flow law, with a uniform temperature of (left column) $T = 0$ °C and (middle column) $T = -2$ °C. The right column shows the difference between the results from the two temperature conditions.

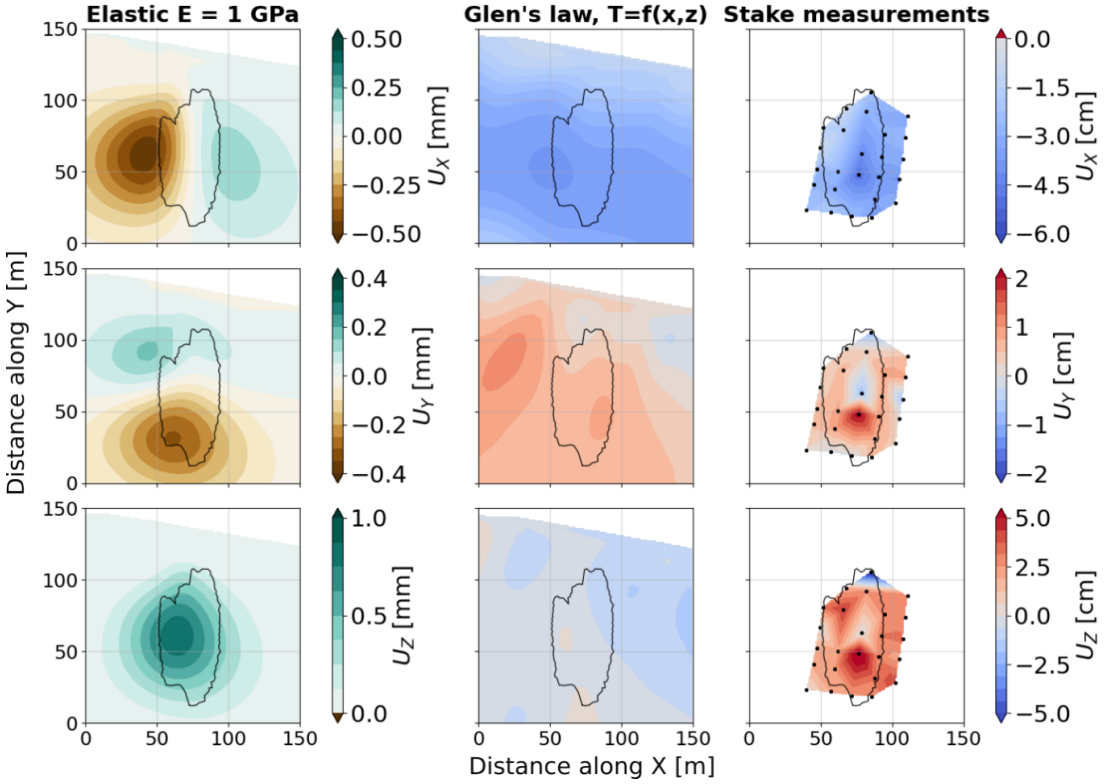

Figure S5. Total displacements in the x (top row), y (middle row) and z (bottom row) directions, obtained from (left) diagnostic simulations based on the linear elastic framework with $E = 1$ GPa, (middle) transient simulation using Glen's law with the spatially distributed T field, and (right) linearly interpolated from total station measurements at stakes between 09 September 2011 and 28 September 2011. Note that displacement units are in millimeters for the elastic case and in centimeters for the other cases. In the right column, black dots indicate positions of stakes. The cavity outline is shown in black.

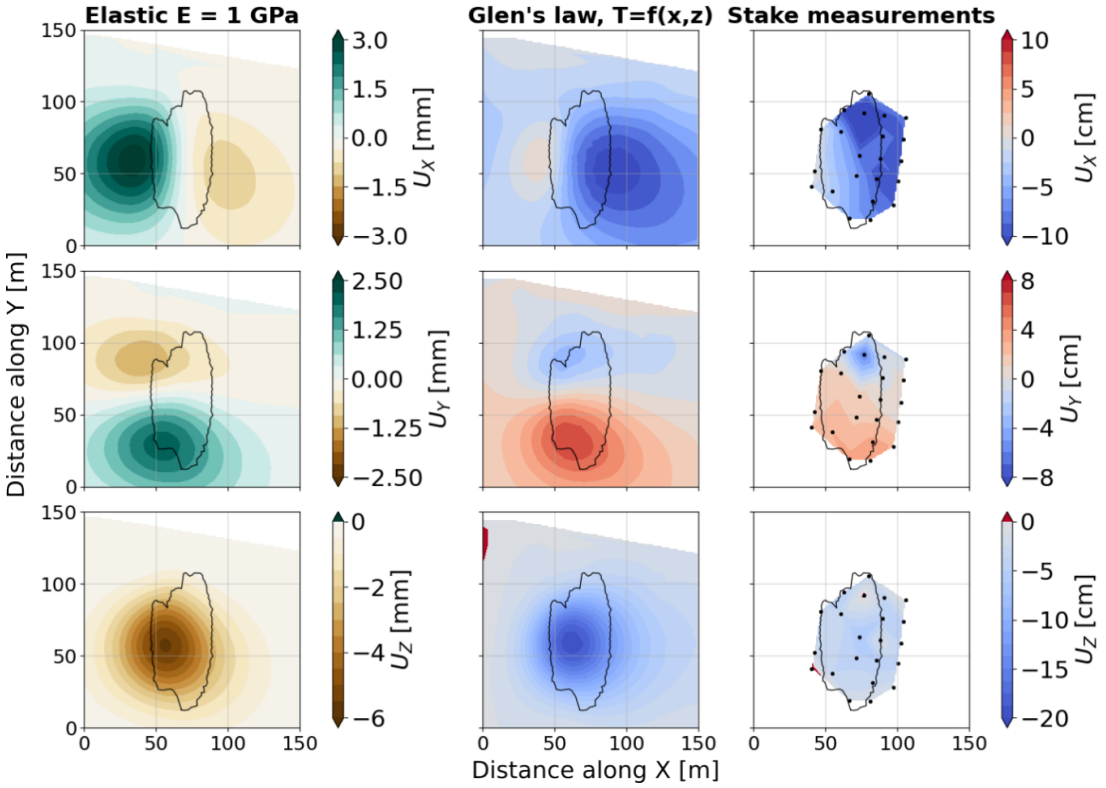

Figure S6. Same as Fig. S5, but for the period from 28 September 2011 to 21 October 2011.

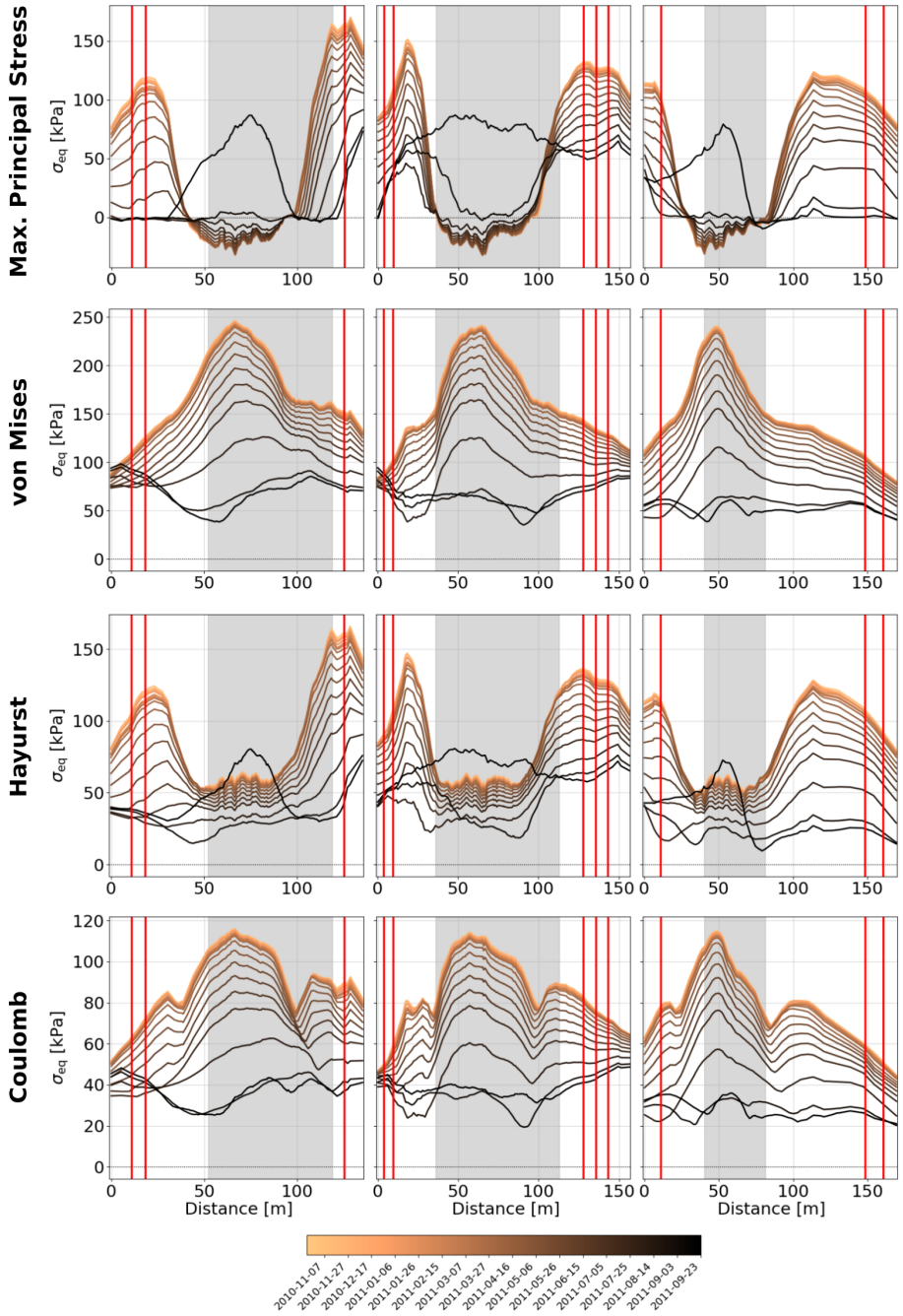

Figure S7. Evolution of surface equivalent stress along transects AA' (left column), BB' (middle column), and CC' (right column) throughout the 2010-2011 refill sequence, for the four failure criteria: MPS (first row), von Mises (second row), Hayhurst (third row), and Coulomb (last row). Although the MPS criterion considers only the positive values of σ_{I} according to Eq. (3) of the main text, negative values are kept here to highlight areas of compressive stresses. Transects are reported in Fig.5 of the main text (white lines). Vertical lines indicate crevasses, while the grey shaded area represents the cavity roof.

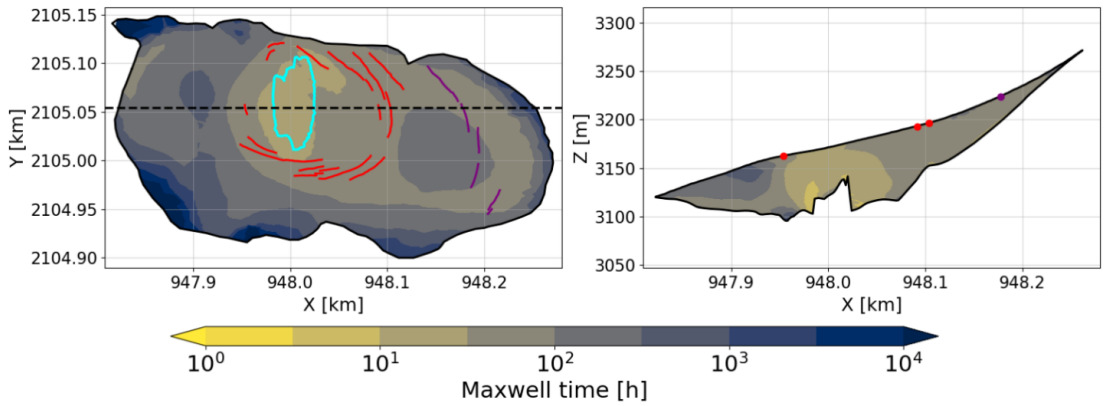

Figure S8. Maxwell time at the glacier surface (left) and across a vertical profile (right) evaluated for an empty cavity according to Eq. (6) of main text with the Glen's law and for $E = 1$ GPa. The cavity contour is shown in cyan. Circular crevasses mapped in summer 2011 are marked in red, while crevasses likely unrelated to cavity drainage are marked in magenta. The transect along which the vertical profile is extracted is reported by the dashed black line in left panel.

References

Gilbert, A., Vincent, C., Wagnon, P., Thibert, E., and Rabatel, A.: The influence of snow cover thickness on the thermal regime of Tête Rousse Glacier (Mont Blanc range, 3200 m a.s.l.): Consequences for outburst flood hazards and glacier response to climate change, Journal of Geophysical Research: Earth Surface, 117, https://doi.org/10.1029/2011JF002258, 2012.